Crystal Structure of HLA-DR2 (DRA*0101, DRB1*1501) Complexed with a Peptide from Human Myelin Basic Protein

By Kathrine J. Smith,*[‡] Jason Pyrdol,[§] Laurent Gauthier,[§]
Don C. Wiley,*[‡] and Kai W. Wucherpfennig[§‖]

From the *Department of Molecular Medicine, Children's Hospital, Boston, Massachusetts 02115; the
[‡]Department of Molecular and Cellular Biology, Harvard University, Cambridge, Massachusetts
02138; the [§]Department of Cancer Immunology and AIDS, Dana-Farber Cancer Institute, Boston,
Massachusetts 02115; and the [‖]Department of Neurology, Harvard Medical School, Boston,
Massachusetts 02115

Summary

Susceptibility to multiple sclerosis is associated with the human histocompatibility leukocyte antigen (HLA)-DR2 (DRB1*1501) haplotype. The structure of HLA-DR2 was determined with a bound peptide from human myelin basic protein (MBP) that is immunodominant for human MBP-specific T cells. Residues of MBP peptide that are important for T cell receptor recognition are prominent, solvent exposed residues in the crystal structure. A distinguishing feature of the HLA-DR2 peptide binding site is a large, primarily hydrophobic P4 pocket that accommodates a phenylalanine of the MBP peptide. The necessary space for this aromatic side chain is created by an alanine at the polymorphic DRβ 71 position. These features make the P4 pocket of HLA-DR2 distinct from DR molecules associated with other autoimmune diseases.

Key words: HLA-DR2 • crystal structure • myelin basic protein • multiple sclerosis • autoimmunity

The MHC region on chromosome 6 represents an important susceptibility locus for a number of polygenic, chronic inflammatory human diseases, such as type I diabetes, rheumatoid arthritis, and multiple sclerosis (MS)[1] (for reviews see references 1–3). In the case of MS, the highest linkage of disease scores within the MHC were obtained with markers for the MHC class II region (4–6). Many previous studies had demonstrated that the DR2 (DRB1*1501) haplotype is present at an increased frequency in patients with MS, in particular in patients of Scandinavian descent who carry the highest risk. This haplotype includes the DRB1*1501, DRB5*0101, DQA1*0102, and DQB1*0602 alleles that are in linkage disequilibrium; these encode HLA-DR2b (DRA, DRB1*1501), HLA-DR2a (DRA, DRB5*0101), and HLA-DQ6 (DQA1*0102, DQB1*0602) (7–9). Disease-associated MHC alleles may confer susceptibility by affecting T cell repertoire selection in the thymus/peripheral immune system and/or by presenting self-peptides against which an autoimmune response is directed. The observation that particular alleles are associated with a given autoimmune disease suggests that a limited number of self-peptides are involved in early stages of the disease process. In later stages of the disease, the autoimmune response may broaden to a larger set of antigens/peptides (epitope spreading; reference 10).

The target antigens in MS are not known; major candidate antigens include myelin basic protein (MBP), proteolipid protein, and myelin oligodendrocyte glycoprotein (MOG). In experimental animal models of MS, central nervous system inflammation and demyelination can be induced by immunization with peptides representing immunodominant T cell epitopes of these antigens or by transfer of antigen-specific T cell clones (for review see reference 11). In addition, antibodies to MOG were shown to enhance demyelination after an inflammatory response had been initiated by myelin-specific T cells (12, 13).

The analysis of the human immune response to myelin antigens has focused primarily on human MBP. A peptide from the middle region of human MBP (residues 84–102) was found to be immunodominant for human MBP-specific T cells, in particular in patients with the HLA-DR2

---

[1]*Abbreviations used in this paper:* HA, hemagglutinin; MBP, myelin basic protein; MS, multiple sclerosis.

haplotype (14–16). MBP(85–99)-specific T cell clones from patients with the HLA-DR2 haplotype were HLA-DR2b (DRA, DRB1*1501) restricted and the peptide was found to bind to purified HLA-DR2b (DRA, DRB1*1501) (17, 18). Val 89 and Phe 92 of the MBP(85–99) peptide were identified as P1 and P4 anchor residues for HLA-DR2b binding. The peptide also bound, with a lower affinity, to HLA-DR2a (DRA, DRB5*0101), with Phe 92 identified as the P1 anchor residue for binding to this MHC class II molecule (17).

Several lines of evidence indicate that MBP-specific T cells are activated and clonally expanded in MS patients. First, *hprt*⁻ mutants reactive to MBP were obtained from blood lymphocytes of MS patients but not control subjects (19). The *hprt*⁻ mutant frequency is higher in cells that have undergone expansion in vivo. Clonal expansion of MBP-specific T cells was also demonstrated by TCR sequence analysis of independent MBP-specific T cell clones from MS patients (20, 21). In addition, T cells specific for the MBP(85–99) peptide could be expanded from the blood of MS patients but not control subjects by stimulation with transfectants that expressed HLA-DR2 but not costimulatory molecules; expansion after MHC/peptide stimulation in the absence of costimulation is a characteristic of memory T cells (22).

We have determined the crystal structure of HLA-DR2 (DRA, DRB1*1501) complexed with a peptide from human MBP. Peptide residues that were previously found to be important for TCR recognition of the MBP peptide are prominent, solvent exposed residues in the HLA-DR2/MBP peptide crystal structure. HLA-DR2 is characterized by a large, primarily hydrophobic P4 pocket, due to the presence of alanine at the polymorphic DRβ71 position. The P4 pocket is occupied by a phenylalanine of the MBP peptide that represents a major anchor residue for HLA-DR2 binding.

Materials and Methods

Protein Expression and Purification. HLA-DR2 (DRA, DRB1*1501) was expressed in the Baculovirus system by replacing the hydrophobic transmembrane regions of DRα and DRβ with leucine zipper dimerization domains from the transcription factors Fos and Jun (23). In the expression construct, the MBP(85–99) peptide sequence was attached to the NH₂ terminus of the mature DRβ chain through a 16–amino acid linker, similar to the strategy described by Kozono et al. (24). The protein was purified from concentrated supernatants by affinity chromatography using mAb L243. The leucine zipper dimerization domains were cleaved from the assembled DR2–MBP peptide complex with V8 protease and the protein was further purified by anion-exchange HPLC.

Protein Crystallization. For crystallization, DR2–MBP was buffer exchanged to 50 mM Tris, pH 7.5, and concentrated to 10 mg/ml in Centricon 10 concentrators (Amicon, Beverly, MA). Crystals were obtained at 18°C in 100 mM glycine, pH 3.5, and 15–18% polyethylene glycol (PEG) 6K. Microseeding was used to improve the quality of the crystals. Crystals (0.3 × 0.2 × 0.1 mm) were harvested for 10–12 h in 30% PEG 6K and 100 mM

glycine, pH 3.5, and were prepared for liquid nitrogen cryo-cooling by slowly transferring individual crystals to harvest buffer containing 5, 10, and 15% ethylene glycol. The final cryoprotectant contained 30% PEG 6K, 15% ethylene glycol, and 100 mM glycine, pH 3.5. Crystals were then flash cooled in cryogenic nitrogen gas for data collection.

Data Collection and Processing. High-resolution data (15–2.6 Å) were collected on beamline A1 at the Cornell High Energy Synchrotron Source (CHESS, Ithaca, NY) (λ = 0.920 Å) using an ADSC 1K CCD detector (0.5° oscillations). Data were indexed and integrated with DENZO (25) and scaled using SCALEPACK (CCP4). Data collection statistics are shown in Table 1. DR2–MBP crystallized in a tetragonal space group with unit cell dimensions $a = b = 95.403$ Å, $c = 295.219$ Å and two molecules per asymmetric unit. Examination of systematic absences identified the space group as either P4₃2₁2 or P4₁2₁2.

Structure Determination and Refinement. The structure was determined by molecular replacement with the program AMoRe (26) using the DR1/hemagglutinin (HA) structure as a search model (27). Before molecular replacement, the HA peptide was removed from the model and 13 polymorphic residues that are different between DR1 and DR2 were changed to alanine. The rotation search gave two different solutions that were related by 180° and represent two noncrystallographically related molecules.

Table 1. *Data Collection and Refinement Statistics*

	Residue	Average B
Crystal space group	P4₃2₁2	
Cell parameters (Å)	$a = b = 95.4; c = 295.2$	
Molecules per ASU	2	
Data Processing		
Resolution limit (Å)	2.6	
Mosaicity (°)	0.48	
R_{merge} (%)	8.8 (27.6)	
Unique reflections	42589	
Total reflections	263333	
Completeness (%)	88.3 (83.1)	
I/σ	23.5 (3.9)	
Refinement		
Data range (Å)	20.0–2.6	
R_{free} (%)	26.6 (38.6)	
R_{cryst} (%)	23.4 (37.7)	
Protein	768	35.6
Water	50	35.7
Root-mean-square-deviations		
Bonds (Å)	0.009	
Angles (°)	1.5	
B factors (Å² bonded)	2.1	

Numbers in parentheses indicate the specific value in the resolution shell from 2.49 to 2.6 Å. A random 5% of reflections were removed for the calculation of R_{free}. $R_{free} = (\Sigma_h|Fo\text{-}Fc|)/(\Sigma_h Fo)$, ∀h ∈ {free set}; $R_{work} = (\Sigma_h|Fo\text{-}Fc|)/(\Sigma_h Fo)$, ∀h ∈ {working set}. $R_{merge} = (\Sigma_{hkl}|I\text{-}<I>|)/(\Sigma_{hkl}<I>)$, ∀ hkl ∈ {independent Miller indices}.

A translation search identified the correct space group enantiomorph as $P4_32_12$ and placed one molecule in the asymmetric unit. This solution was fixed and used to place the second molecule in the asymmetric unit. The two molecules are related by an approximate twofold noncrystallographic axis. Rigid body refinement of the molecular replacement solution in XPLOR (data 10–3.0 Å) yielded $R_{free} = 40.2\%$, $R_{work} = 39.6\%$.

Refinement was carried out using version 3.851 of XPLOR (28). A bulk solvent correction was calculated to allow the inclusion of data from 20 Å resolution in the refinement procedure. Cycles of manual model building in O (29) and refinement in XPLOR were carried out, during which DR2 polymorphic residues and the MBP peptide were built into the model and data was included to 2.6 Å. The refinement protocol involved positional refinement with noncrystallographic symmetry restraints, group B factor refinement for data from 20 to 3.0 Å resolution, and restrained individual B factor refinement for data from 20 to 2.6 Å resolution. The model was built into 2Fo-Fc and Fo-Fc electron density maps. Maps were improved by solvent flattening and averaging across the noncrystallographic twofold symmetry axis. The peptide (P-4 to P9) was built into clear, unambiguous density when $R_{free} = 32.5\%$ and $R_{work} = 25.9\%$; after addition of the peptide, $R_{free} = 28.1\%$ and $R_{work} = 24.6\%$. Crystallographic restraints were lifted for the final two rounds of refinement. The final model ($R_{free} = 26.6\%$, $R_{work} = 23.4\%$) contains 768 residues, 50 water molecules, and 2 sugar molecules (attached to residue Asn α118 of both NCS-related molecules). No density was observed for the covalent linker. Electron density at the COOH terminus of the peptide (P10 and P11) is weak, indicating that this region of the peptide is partially disordered. Analysis of ϕ ψ angles shows that 85.9% of residues have most favored angles, 12.9% (87 residues) have additionally allowed angles, 0.7% (5 residues) have generously allowed angles, and 0.3% (2 residues) have disallowed angles (30). Refinement statistics are shown in Table 1.

Results

Determination of the Structure of HLA-DR2–MBP Peptide Complex. The structure of HLA-DR2 complexed with a peptide from human MBP (residues 85–99) was determined to 2.6 Å resolution by x-ray crystallography (see Materials and Methods). The complex was produced using a Baculovirus insect cell expression system with the MBP peptide covalently linked to the NH_2 terminus of the mature DR2 β chain, as described by Kozono et al. for murine MHC class II molecules (24). The protein also included COOH-terminal leucine zipper dimerization domains that were proteolytically cleaved before crystallization (23). The complex crystallized in a tetragonal space group ($P4_32_12$) with two molecules per asymmetric unit. The two molecules are related by an approximate twofold noncrystallographic symmetry axis (177.5°) resulting in the formation of a dimer similar to that previously observed for HLA-DR1 and HLA-DR3 (27, 31, 32). Crystallographic statistics are shown in Table 1.

General Features of the HLA-DR2 Peptide-binding Site. HLA-DR2 differs from HLA-DR4, which is associated with susceptibility to rheumatoid arthritis, at 10 positions within the β1 domain (Table 2, reference 33). These polymorphisms affect the specificity of the P1, P4, P6, P7, and

Table 2. *DRβ Chain Residues that Differ between HLA-DR2 and HLA-DR4*

DRβ chain residue	Pocket	HLA-DR2	HLA-DR4
		(DRB1*1501)	(DRB1*0401)
9	P9	Trp	Glu
11	P6	Pro	Val
13	P6,P4	Arg	His
33	–	Asn	His
37	–	Ser	Tyr
47	P7	Phe	Tyr
67	–	Ile	Leu
71	P7, P4	**Ala**	Lys
86	P1	Val	Gly
96	–	Gln	Tyr

P9 pockets. Of particular importance is the contribution of DRβ71 to the shape and charge of the P4 pocket, as discussed below. The MBP peptide is bound in the binding groove of DR2 with peptide side chains P1, P4, P6, and P9 occupying pockets within the groove (Fig. 1 *A*). The P1 and P4 pockets are occupied by valine 89 and phenylalanine 92, respectively, of the MBP(85–99) peptide. Peptide binding experiments with single amino acid analogues had demonstrated that these two residues represent the main anchor residues for DR2 binding. Residues P2, P3, and P5 (histidine, phenylalanine, and lysine) were identified as major TCR contact residues for human MBP-specific T cell clones (17), and in the crystal structure reported here were observed to be solvent exposed and accessible for recognition by TCR (Fig. 1, *B* and *D*).

Overall Conformation of the HLA-DR2–bound MBP Peptide. The model for the MBP peptide (85–99) includes residues 86–99 on one DR2 molecule and residues 85–98 on the second DR2 molecule in the asymmetric unit of the crystal (Fig. 2 *B, yellow* and *blue,* respectively). Electron density is weak for residues P10 and P11 of the peptides, suggesting that the COOH termini of the two peptides are partially disordered (Fig. 2 *A*). A crystal contact between peptide residue P-3 in one molecule and P5 from a molecule with related symmetry stabilizes the NH_2 terminus of one peptide, enabling P-4 to be included in the model for this peptide and P5 lysine to be included in the model for the other peptide. Analysis of MBP-specific T cell clones demonstrated that truncation of the P-4 residue (glutamic acid) greatly reduced the stimulatory capacity of the MBP peptide for some of the human T cell clones, indicating that the peptide NH_2 terminus may interact with the TCR (17). However, the arching up of residues P-3 and P-4 in the DR2/MBP peptide structure may not represent the position of these residues in a HLA-DR2–MBP-peptide–TCR complex, but instead a conformation stabilized by the crystal contact. The two noncrystallographically related
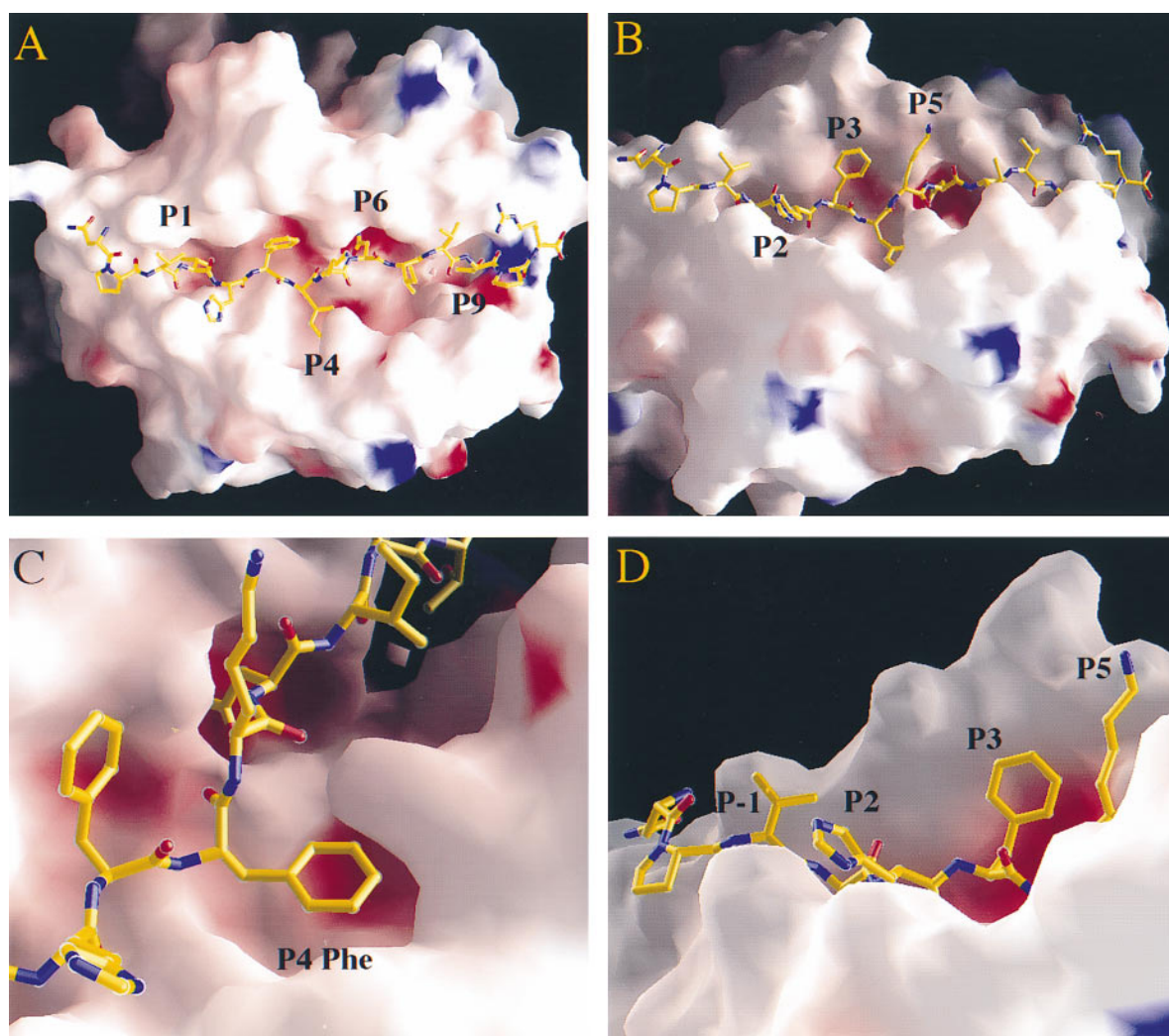
Figure 1. Overall structure of the HLA-DR2–MBP peptide complex. (*A* and *B*) Top and side view of the HLA-DR2–MBP peptide complex. 14 residues are included for the MBP peptide (P-3 Asn to P11 Arg). P1 Val and P4 Phe occupy the hydrophobic P1 and P4 pockets, respectively, and serve as primary anchor residues of the MBP peptide. Peptide atoms are shown as ball-and-stick. (*C*) View of the large P4 pocket of HLA-DR2 that is occupied by P4 Phe of the MBP peptide. Gln β70 is positioned over P4 Phe of the peptide. (*D*) TCR contact residues of the MBP peptide. P2 His, P3 Phe, and P5 Lys that were previously shown to be important for TCR recognition of the MBP peptide are prominent, solvent exposed residues. Figure was drawn with GRASP (55).

peptides vary slightly in conformation from P6 to P10, where they are influenced by different crystal contacts to the β2 helix. Specifically, for one molecule in the asymmetric unit there is a crystal contact of Arg α50 on a symmetry related molecule with Asp β66, Gln β64, Tyr β60, and P6 Ile.

The overall conformation of the MBP peptide in the DR2 binding groove is similar to that observed for other HLA-DR–peptide complexes (27, 31, 32, 34; Fig. 3). Superposition of MHC class II peptides shows that the main chain conformation is highly conserved for the NH$_2$-terminal segment of these peptides (P-1 to P4); this segment carries the main DR2 anchor residues (P1 and P4) as well as important TCR contact residues of the MBP peptide (histidine and phenylalanine at P2 and P3, as well as lysine at P5). The conformation of MHC class II–bound peptides is more divergent towards the COOH-terminal segment (P6–P10), as described in Dessen et al. (34). Fig. 3 shows that the COOH terminus of the MBP peptide is positioned higher in the peptide binding groove than other human and murine peptides.

HLA-DR2 Binding and TCR Contact Residues in the NH$_2$ Terminus of the MBP Peptide. The NH$_2$ terminus of the peptide (P-3 to P4) is held in the DR2 peptide binding groove by a conserved network of hydrogen bonds (27). Residue P-3 of the peptide is stabilized by an additional hydrogen bond from the NH of the P-3 side chain to Ser α53 Oγ. Valine at the P1 position of the MBP peptide occupies the hydrophobic P1 pocket. Val β86 at the base of the P1 pocket results in a smaller P1 pocket than that observed for DR1 and DR4 (Gly at β86), creating a hydrophobic pocket identical to that reported for DR3 (31),
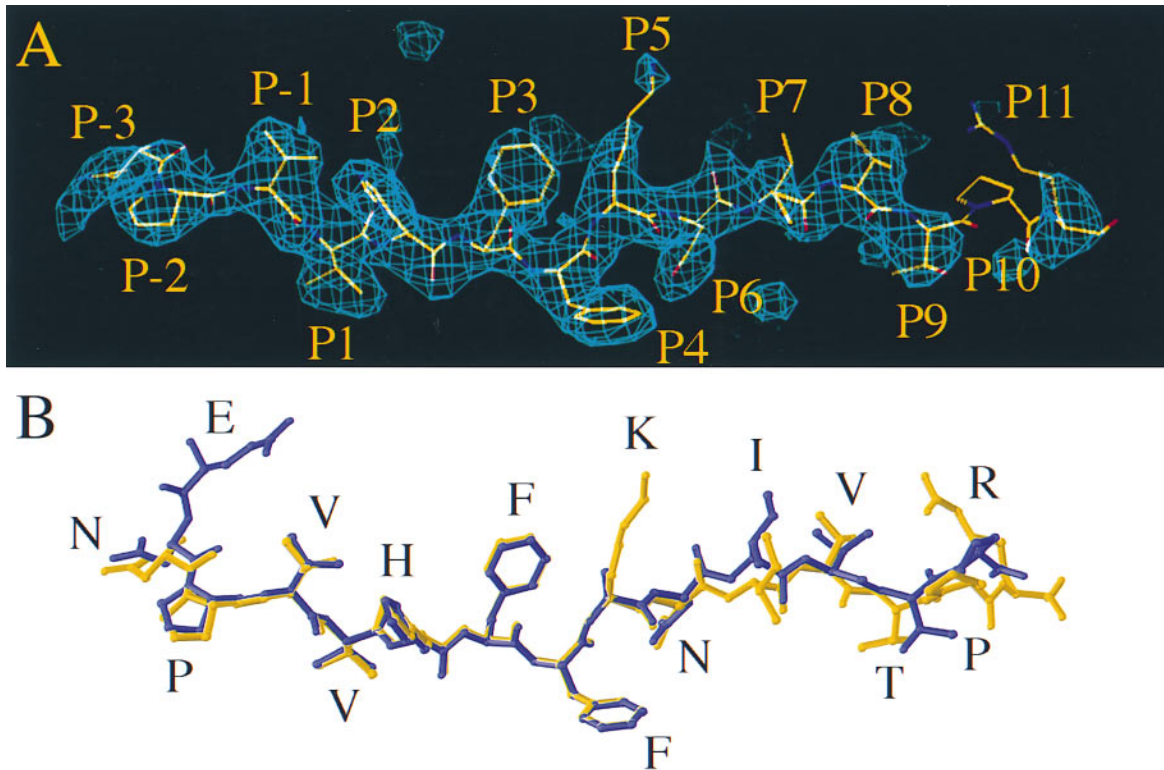
Figure 2. (*A*) Electron density of the MBP peptide bound to HLA-DR2. Fo-Fc omit map of the peptide. The COOH terminus of the peptide (P10, P11) is partially disordered. (*B*) Superposition of the two MBP peptides in the asymmetric unit. The model for the MBP peptide includes residues P-3 to P11 and P-4 to P10 for the two copies in the asymmetric unit (*yellow* and *blue*, respectively). The peptide backbones superimpose in the P-1 to P4 segment and are more divergent in the COOH-terminal segment due to different crystal contacts to the β2 helix. A crystal contact between peptide residue P-3 in one molecule and P5 from a symmetry related molecule stabilizes the NH$_2$ terminus of one peptide, enabling P-4 to be included in the model for this peptide and P5 Lys to be included in the model for the other peptide. Figure was drawn with RIBBONS (56).

which can bind aliphatic amino acids and phenylalanine (35). Residue P2 His of the MBP peptide packs against His β81, whereas side chain P3 Phe nestles in a hydrophobic shelf of the α2 helix. The side chains of P2 His and P3 Phe are both accessible for interaction with the TCR (Fig. 1, *A–D*). The peptide main chain from P-3 to P4 of the MBP peptide superimposes almost identically with the main chain of other peptides bound to human DR molecules (Fig. 3), probably because these DR molecules are identical in this part of the groove; the only polymorphism in this region is at position β86 at the bottom of the P1 pocket.

The Large, Primarily Hydrophobic P4 Pocket of HLA-DR2. In the HLA-DR2–MBP peptide complex, the P4 pocket is occupied by an aromatic side chain (Phe) that makes an important contribution to the binding of the MBP peptide. The P4 pocket of HLA-DR2 has a preference for aromatic as well as aliphatic residues. Binding is also observed with analogues of the MBP peptide that carry a substitution by histidine, arginine, lysine, glutamine or asparagine at P4; substitution by aspartic acid is not tolerated (reference 17 and Pyrdol, J., and K.W. Wucherpfennig, unpublished data). In contrast, HLA-DR4 has a preference for negatively charged residues, hydrogen bond donors, and some aliphatic amino acids at P4; peptides with aromatic or posi-

tively charged residues at P4 bind poorly (36, 37). DR2 and DR4 differ only at two positions in the P4 pocket, β71 (Ala in DR2, Lys in DR4) and β13 (Arg in DR2, His in DR4) (Table 2 and Fig. 4).

The structural basis for this side chain specificity is clear from the DR2–MBP structure, which reveals a large, predominantly hydrophobic P4 pocket (Figs. 1 *C* and 5 *A*). The pocket is lined by two aromatic MHC side chains, Tyr β78 and Phe β26, as well as side chains Gln β70, Ala β71, Asp β28, and Arg β13. The polymorphism at position 71 in DR2 (Ala) appears to be most important in creating the available space for the P4 aromatic side chain (Phe) of the MBP peptide. The presence of negatively charged Asp β28 at the base of the pocket would allow the binding of positively charged side chains but be unfavorable for the binding of negatively charged side chains.

In contrast, the P4 pocket of DR4 is smaller and carries a positive charge at DRβ71. In the crystal structure of DR4 with a bound type II collagen peptide, a salt bridge was present between an aspartic acid residue of the peptide and Lys β71 (reference 34; Fig. 5 *B*). Since the majority of DRB1 alleles encode lysine, arginine, or glutamic acid at DRβ71 (33), the binding of aromatic side chains is an important aspect of the DR2 peptide binding specificity.
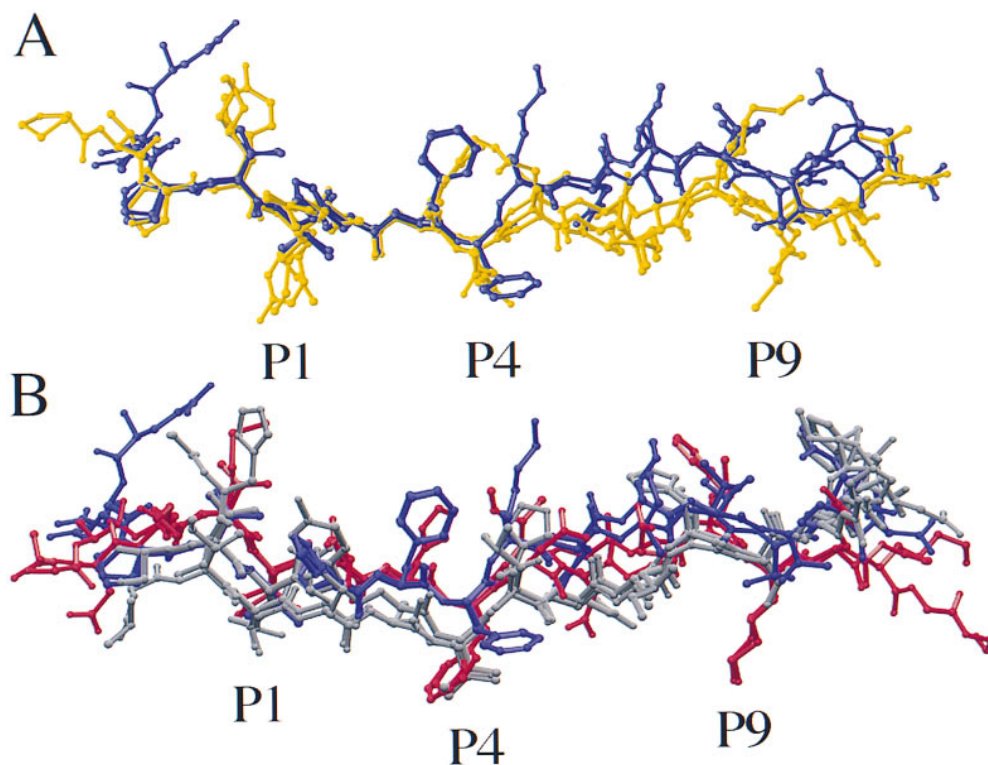
Figure 3. Superposition of human and murine MHC class II–bound peptides. (*A*) Superposition of the two MBP peptides in the asymmetric unit (*blue*) and peptides bound to other human MHC class II molecules (*yellow*). Human MHC class II peptides: DR1–HA, DR3–CLIP, DR4–type II collagen (27, 32, 34). The conformation of the peptide backbone is highly conserved in the P-1 to P4 segment and divergent in the COOH-terminal segment. (*B*) Superposition of the two MBP peptides in the asymmetric unit (*blue*) and murine MHC class II peptides. I-E^k peptides (I-E^k/Hb, I-E^k/Hsp) are in red and I-A peptides (I-A^k/HEL, I-A^d/Ova, I-A^d/HA) are in gray (39–41). The conformation of the peptide backbone is similar between HLA-DR and I-E molecules in the P1 to P4 segment. I-A peptides are bound deeper in the peptide binding site than DR or I-E peptides. Superpositions were carried out using the α1 and β1 domains of MHC class II molecules. Figure was drawn with RIBBONS (56).

The DRβ71 polymorphism, which is not solvent exposed, has also been reported to affect TCR recognition of DR–peptide complexes (38). The indirect effect of DRβ71 on TCR recognition can be understood by comparison of the P4 pockets of DR2 and DR4 (Fig. 5), which shows that solvent-exposed MHC residue Gln β70 differs markedly in its position between the two structures. In the DR2–MBP peptide structure, Gln β70 is in a horizontal position relative to the peptide binding site while it is pointing up in the DR4–type II collagen peptide structure. These results indicate that DRβ71 can have an indirect effect on TCR recognition by altering the characteristics of the P4 pocket and the interactions that a bound peptide anchor residue can make with solvent accessible side chains.

COOH Terminus of the MBP Peptide. The COOH-terminal half of the peptide main chain, from P5 to P10, is positioned higher in the groove than peptides bound to DR1, DR3, and DR4 (Fig. 3). P6 Asn of the MBP peptide binds in a polar P6 pocket (Fig. 1, *A* and *C*), forming part of a complex hydrogen bonding network that includes conserved MHC side chains Glu α11, Asn α69, Asn α62, Asp α66, a water molecule, and polymorphic residue Arg β13. The nature of this pocket is likely to be conserved in all human DR and mouse I-E molecules and has been suggested to determine the pH dependency of MHC class II peptide loading (39). Single amino acid substitutions of the MBP peptide show that analogues with a negatively charged side chain bind poorly at P6 (Pyrdol, J., and K.W. Wucherpfennig, unpublished data). This is readily ex-

plained by the DR2–MBP crystal structure, which reveals a predominantly negatively charged pocket (Fig. 1, *A* and *C*). Available space in the polar P6 pocket is limited compared with other DR alleles due to the presence of polymorphic side chain Arg β13. This prevents P6 Asn from binding as deeply in the P6 pocket as previously observed for DR–peptide complexes and is at least partially responsible for the raised position of the MBP peptide COOH terminus within the peptide binding groove.

Peptide side chains P7 Ile and P9 Thr do not fully occupy the available space in their binding pockets (Fig. 1, *A* and *C*). Two water molecules fill the space usually occupied by the P7 side chain. It would appear to be more energetically favorable for the polar P7 pocket to be filled with water molecules than the hydrophobic P7 Ile peptide side chain. The water molecules are satisfying hydrogen bonding requirements (particularly of residues Asp β28 and Tyr β30) that could not be satisfied by P7 Ile. The hydrophobic DR2 P9 pocket is identical to the DR1 P9 pocket. However, the MBP peptide P9 Thr does not fully occupy the available space in the P9 pocket (Fig. 1, *A* and *B*). It is possible that this is due to the suboptimal nature of the P9 anchor residue since substitution of the P9 position results in a modest increase of the binding affinity of the MBP peptide (reference 17 and Pyrdol, J., and K.W. Wucherpfennig, unpublished data). Also, the position of P9 Thr could be due to the overall raised position of the COOH terminus of the MBP peptide within the DR2 binding groove that prevents P9 Thr from binding more deeply in the P9
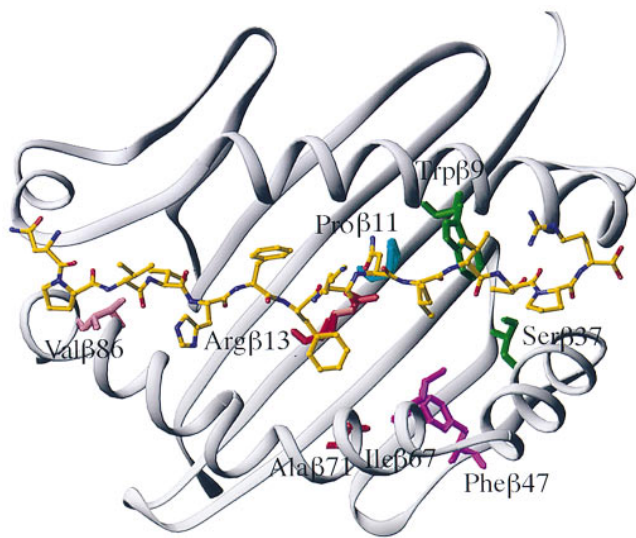
Figure 4. DRβ chain residues that differ between HLA-DR2 and HLA-DR4. The HLA-DR2 peptide binding groove is viewed from above with the MBP peptide represented in yellow as a ball-and-stick model. Polymorphic side chains that are different between DR2 and DR4 are shown and color coded according to their proximity to a peptide binding pocket. Color coding: *pink*, P1 pocket; *red*, P4 pocket; *blue*, P6 pocket; *magenta*, P7 pocket; *green*, P9 pocket. Arg β13 (*red*) forms part of both the P4 and P6 pockets. Asn β33 and Gln β96 are not located within the immediate vicinity of the peptide and are not included in the figure. Figure was drawn with RIBBONS (56).

pocket. The raised position of the peptide COOH terminus compared with other DR–peptide complexes therefore may be due to a relatively poor fit of the peptide side chains to the available pockets.

A contribution by the covalent linker on the position of the COOH terminus of the peptide cannot be excluded. In this respect it is interesting to compare the DR2–MBP structure with the mouse I-E^k, I-A^k, and I-A^d crystal structures that were also determined with peptides covalently linked to the NH$_2$ terminus of the class II β chain. In the I-E^k structures, the covalent linker is ordered, positions P9 and P10 of the peptide are not raised, and anchor residue P9 Lys binds deep in the P9 pocket (39). However, for the peptides bound to the I-A structures, the linkers are disordered, the P9 anchor residue is small, and the peptide COOH terminus is raised in the groove (40, 41). These results suggest the possibility that in the case where the P9 residue is small, the presence of a covalent linker may influence the position of the peptide COOH terminus.

In addition to the partial occupancy of the P7 and P9 pockets, the hydrogen bonding pattern at the COOH terminus of the MBP peptide is unusual. Hydrogen bonds from conserved MHC residue Trp β61 to peptide P8 O and residue α69 to peptide P9 N and P7 O are not formed. Similarly, the hydrogen bond from Trp β61 to P8 O is absent in the I-A^k/hen egg lysozyme structure (40). The observation that the P7 and P9 pockets are only partially occupied is consistent with peptide binding studies. The COOH terminus of the MBP peptide could be truncated to P7 Ile without a significant loss of binding affinity (17),

and substitutions at P6, P7, or P9 of the MBP peptide had relatively little effect on DR2 binding. Taken together, these data indicate that the peptide COOH terminus does not contribute significantly to the overall binding energy of the MBP peptide to HLA-DR2.

Discussion

Previous studies demonstrated that P2 His, P3 Phe, and P5 Lys are important residues for TCR recognition of the DR2–MBP peptide complex (17, 42). The DR2–MBP crystal structure shows that these peptide side chains are solvent exposed (Fig. 1 *D*) and available for TCR recognition. Comparison with the recently published high resolution crystal structures of human MHC class I–peptide–TCR complexes (43, 44) suggests that P5 Lys would bind in a pocket formed between the TCR Vα and Vβ domains and may form a hydrogen bond to negatively charged residue(s) in the CDR3 loop of α and/or β.

P3 Phe is a primary TCR contact residue for human MBP(85–99)-specific T cell clones since substitution of P3 Phe reduces/abolishes T cell activation without affecting DR2 binding. Some T cell clones are highly specific for this position since substitution by any natural amino acid greatly reduces or abolishes T cell activation. The NH$_2$-terminal segment of the MBP peptide makes a contribution to TCR recognition since truncation of P-4 and P-3 greatly diminishes TCR recognition by some DR2–MBP-specific T cell clones without affecting DR2 binding. In contrast, the COOH-terminal segment of the peptide is not important for recognition by these T cell clones since almost all substitutions at P7, P8 and P9 are tolerated (reference 17 and Pyrdol, J., and K.W. Wucherpfennig, unpublished data). The degenerate HLA-DR2 binding motif as well as the requirement for sequence similarity/identity at a limited number of peptide residues that interact with the TCR account for the observation that microbial peptides that are quite diverse in their primary sequence can activate human MBP-specific T cell clones (42, 45).

A large, primarily hydrophobic P4 pocket was found to be a prominent feature of the DR2 peptide binding site. This pocket is occupied by a phenylalanine of the MBP peptide that makes an important contribution to the binding of the MBP peptide to DR2. The presence of an alanine at the polymorphic DRβ71 position creates the necessary room for the binding of an aromatic side chain in the P4 pocket. The binding of aromatic side chains by the P4 pocket of DR2 is also facilitated by two aromatic residues of the P4 pocket (β26 Phe and β78 Tyr, of which β26 is polymorphic) (Fig. 5 *A*). The presence of alanine at DRβ71 is unusual for DRB1 alleles and has only been observed for DR2 alleles (DRB1*1501-DRB1*1506) and DRB1*1309; all other known DRB1 alleles encode lysine, arginine, or glutamic acid at this position (33). In Caucasians, DRB1*1501 is the most common DR2 haplotype; it is also the haplotype that confers an increased susceptibility to the development of MS. It is not known if other DR2 alleles confer susceptibility to MS because they are rela-
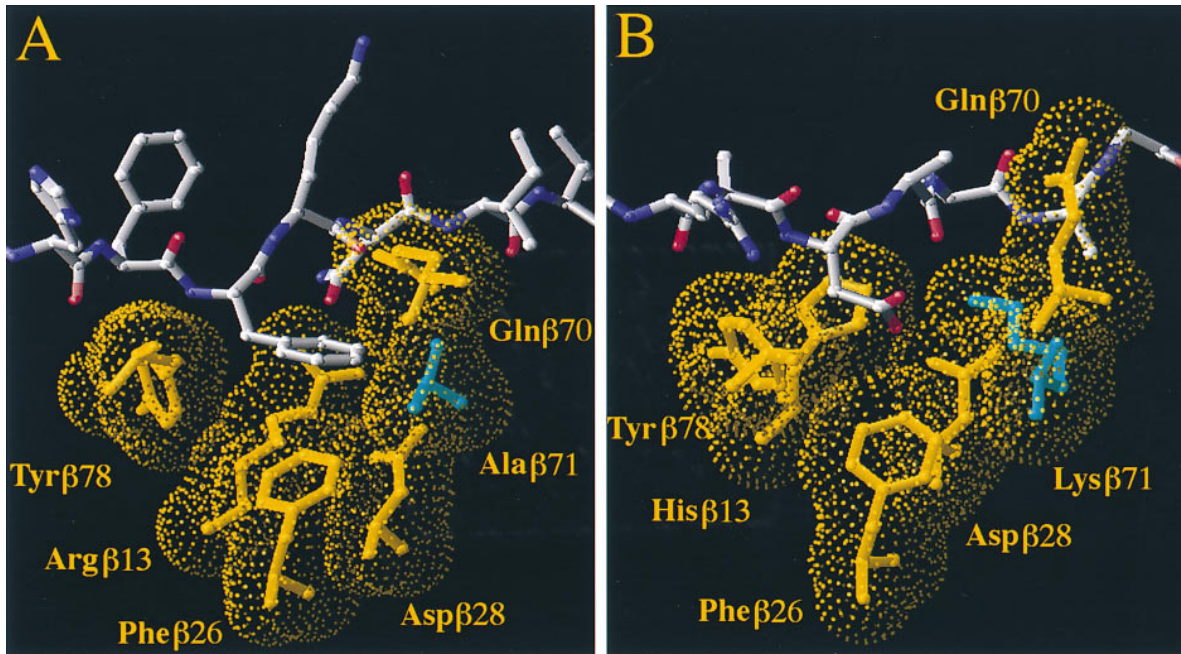
Figure 5. Comparison of the P4 pockets of HLA-DR2 and HLA-DR4. (*A*) P4 pocket of HLA-DR2. P4 Phe of the MBP peptide occupies a large, predominantly hydrophobic pocket in HLA-DR2. P4 Phe interacts with another aromatic residue, Phe β26. The fact that the polymorphic DRβ71 residue is an alanine (*blue*) creates the necessary space for the aromatic peptide side chain. Gln β70 is in an approximately horizontal position. (*B*) P4 pocket of HLA-DR4. DRβ71 is a lysine (*blue*) and makes a salt bridge to P4 Asp of the type II collagen peptide (34). Gln β70 is rotated to a more upward pointing position. Figure was drawn with RIBBONS (56).

tively uncommon in Europe and Northern America, where the highest prevalence of MS is observed. Since the DRB1 gene is in linkage disequilibrium with the DRB5 gene as well as DQA/DQB genes, both DR and DQ molecules encoded by this haplotype may contribute to the pathogenesis of MS (9).

The P4 pocket of HLA-DR makes an important contribution to susceptibility to other human autoimmune diseases. This is readily explained by the fact that the P4 pocket is the most polymorphic pocket of the HLA-DR binding site. For example, an HLA-DR4 allele (DRB1*0402) that is associated with susceptibility to pemphigus vulgaris, an autoimmune disease of the skin, differs from a rheumatoid arthritis associated allele (DRB1*0404) only at three positions, DRβ67, -70, and -71. In the pemphigus vulgaris associated allele, DRβ70 and -71 of the P4 pocket carry negative charges (aspartic acid and glutamic acid, respectively). In contrast, glutamine and lysine/arginine are present at DRβ70 and -71, respectively, in rheumatoid arthritis–associated alleles (DRB1*0401 and *0404) (2, 37, 46–49). A peptide from type II collagen that is immunodominant for murine type II collagen–specific T cells has been identified in HLA-DR1 and HLA-DR4 transgenic mice; this peptide carries an aspartic acid residue at the P4 position (50, 51).

The structural characteristics of the DR2 binding site may also help to explain the binding of Cop 1 to DR2 and other DR molecules. Cop 1 is a random copolymer composed of l-alanine, l-lysine, l-glutamic acid, and l-tyrosine in a molar ratio of 6.0:4.7:1.9:1.0 that has shown a certain degree of clinical efficacy in relapsing-remitting MS (52, 53). Cop 1 was found to bind to a number of different DR molecules and to compete with the binding of peptides (54). Since DR1 (DRA, DRB1*0101) and DR4 (DRA, DRB1*0401) have large P1 pockets (Gly at β86), tyrosine may serve as a P1 anchor for DR1 and DR4 binding. In contrast, the P1 pocket of HLA-DR2 is too small (Val at β86) to accommodate a tyrosine side chain and too hydrophobic to accommodate lysine or glutamic acid. It is more likely that a tyrosine residue of Cop 1 could be accommodated in the P4 pocket of DR2 and act as an anchor residue for Cop 1 binding.

The structural information on the P4 pocket of different DR molecules may be useful for the development of small organic molecules that inhibit peptide presentation by DR molecules associated with particular autoimmune diseases. Introduction of particular moieties in the P4 pocket may allow specificity for certain DR molecules to be introduced. For example, ligands with large, aromatic substituents in the P4 pocket may be relatively selective for DR2, whereas a negatively charged substituents may introduce a certain degree of specificity for rheumatoid arthritis–associated DR4 molecules.

References

1. Todd, J.A., H. Acha-Orbea, J.I. Bell, N. Chao, Z. Fronek, C.O. Jacob, M. McDermott, A.A. Sinha, L. Timmerman, L. Steinman, and H.O. McDevitt. 1988. A molecular basis for MHC class II–associated autoimmunity. *Science.* 240:1003–1009.

2. Nepom, G.T., and H. Erlich. 1991. MHC class-II molecules and autoimmunity. *Annu. Rev. Immunol.* 9:493–525.

3. Davies, J.L., Y. Kawaguchi, S.T. Bennett, J.B. Copeman, H.J. Cordell, L.E. Pritchard, P.W. Reed, S.C.L. Gough, S.C. Jenkins, S.M. Palmer, et al. 1994. A genome-wide search for human type I diabetes susceptibility genes. *Nature.* 371:130–136.

4. The Multiple Sclerosis Study Group. 1996. A complete genomic screen for multiple sclerosis underscores a role for the major histocompatibility complex. *Nat. Genet.* 13:469–471.

5. Sawcer, S., H.B. Jones, R. Feakes, J. Gray, N. Smaldon, J. Chataway, N. Robertson, D. Clayton, P.N. Goodfellow, and A. Compston. 1996. A genome screen in multiple sclerosis reveals susceptibility loci on chromosome 6p21 and 17q22. *Nat. Genet.* 13:464–468.

6. Ebers, G.C., K. Kukay, D.E. Bulman, A.D. Sadovnick, G. Rice, C. Anderson, H. Armstrong, K. Cousin, R.B. Bell, W. Hader, et al. 1996. A full genome search in multiple sclerosis. *Nat. Genet.* 13:472–476.

7. Spielman, R.S., and N. Nathenson. 1982. The genetics of susceptibility to multiple sclerosis. *Epidemol. Rev.* 4:45–65.

8. Hillert, J., T. Kall, M. Vrethem, S. Fredrikson, M. Ohlson, and O. Olerup. 1994. The HLA-Dw2 haplotype segregates closely with multiple sclerosis in multiplex families. *J. Neuroimmunol.* 50:95–100.

9. Oksenberg, J.R., E. Seboun, and S.L. Hauser. 1996. Genetics of demyelinating diseases. *Brain Pathol.* 6:289–302.

10. Lehmann, P.V., T. Forsthuber, A. Miller, and E.E. Sercarz. 1992. Spreading of T-cell autoimmunity to cryptic determinants of an autoantigen. *Nature.* 358:155–157.

11. Steinman, L. 1996. Multiple sclerosis: a coordinated immunological attack against myelin in the central nervous system. *Cell.* 85:299–302.

12. Linington, C., M. Bradl, H. Lassmann, C. Brunner, and K. Vass. 1988. Augmentation of demyelination in rat acute allergic encephalomyelitis by circulating mouse monoclonal antibodies directed against a myelin/oligodendrocyte glycoprotein. *Am. J. Pathol.* 130:443–454.

13. Schluesener, H.J., R.A. Sobel, C. Linington, and H.L. Weiner. 1987. A monoclonal antibody against a myelin oligodendrocyte glycoprotein induces relapses and demyelination in central nervous system autoimmune disease. *J. Immunol.* 139:4016–4021.

14. Ota, K., M. Matsui, E.L. Milford, G.A. Mackin, H.L. Weiner, and D.A. Hafler. 1990. T-cell recognition of an immunodominant myelin basic protein epitope in multiple sclerosis. *Nature.* 346:183–187.

15. Pette, M., K. Fujita, D. Wilkinson, D.M. Altmann, J. Trowsdale, G. Giegerich, A. Hinkkanen, J.T. Epplen, L. Kappos, and H. Wekerle. 1990. Myelin autoreactivity in multiple sclerosis: recognition of myelin basic protein in the context of HLA-DR2 products by T lymphocytes of multiple sclerosis patients and healthy donors. *Proc. Natl. Acad. Sci. USA.* 87:7968–7972.

16. Martin, R., D. Jaraquemada, M. Flerlage, J. Richert, J. Whitaker, E.O. Long, D.E. McFarlin, and H.F. McFarland. 1990. Fine specificity and HLA restriction of myelin basic protein–specific cytotoxic T cell lines from multiple sclerosis patients and healthy individuals. *J. Immunol.* 145:540–548.

17. Wucherpfennig, K.W., A. Sette, S. Southwood, C. Oseroff, M. Matsui, J.L. Strominger, and D.A. Hafler. 1994. Structural requirements for binding of an immunodominant myelin basic protein peptide to DR2 isotypes and for its recognition by human T cell clones. *J. Exp. Med.* 179:279–290.

18. Valli, A., A. Sette, L. Kappos, C. Oseroff, J. Sidney, G. Miescher, M. Hochberger, E.D. Albert, and L. Adorini. 1993. Binding of myelin basic protein peptides to human histocompatibility leukocyte antigen class II molecules and their recognition by T cells from multiple sclerosis patients. *J. Clin. Invest.* 91:616–628.

19. Allegretta, M., J.A. Nicklas, S. Sriram, and R.J. Albertini. 1990. T cells responsive to myelin basic protein in patients with multiple sclerosis. *Science.* 247:718–721.

20. Wucherpfennig, K.W., J. Zhang, C. Witek, M. Matsui, K. Ota, and D.A. Hafler. 1994. Clonal expansion and persistence of human T cells specific for an immunodominant myelin basic protein peptide. *J. Immunol.* 150:5581–5592.

21. Vandevyver, C., N. Mertens, P. van den Elsen, R. Medaer, J. Raus, and J. Zhang. 1995. Clonal expansion of myelin basic protein-reactive T cells in patients with multiple sclerosis: restricted T cell receptor V gene rearrangements and CDR3 sequence. *Eur. J. Immunol.* 25:958–968.

22. Scholz, C., K.T. Patton, D.E. Anderson, G.J. Freeman, and D.A. Hafler. 1998. Expansion of autoreactive T cells in multiple sclerosis is independent of exogenous B7 costimulation. *J. Immunol.* 160:1532–1538.

23. Kalandadze, A., M. Galleno, L. Foncerrado, J.L. Strominger, and K.W. Wucherpfennig. 1996. Expression of HLA-DR2 molecules: replacement of the hydrophobic transmembrane region by a leucine zipper dimerization motif allows the assembly and secretion of soluble DR $\alpha\beta$ heterodimers. *J. Biol.*

Chem. 271:20156–20162.

24. Kozono, H., J. White, J. Clements, P. Marrack, and J.W. Kappler. 1994. Functional soluble major histocompatibility proteins with covalently bound peptides. *Nature.* 369:151–154.

25. Otwinowski, Z. 1993. Data collection and processing. *In* Proceedings of CCP4 Study Weekend. L. Sawyer, N. Isaacs, and S. Bailey, editors. SERC Daresbury Laboratory, Warrington, UK. 56–62.

26. Navaza, J. and P. Saludjian. 1997. AMoRe: an automated molecular replacement program package. *Methods Enzymol.* 276:581–594.

27. Stern, L.J., J.H. Brown, T.S. Jardetzky, R. Urban, J.L. Strominger, and D.C. Wiley. 1994. Crystal structure of the human class II MHC protein HLA-DR1 complexed with an influenza virus peptide. *Nature.* 368:215–221.

28. Brünger, A.T. 1992. Free R value: a novel statistical quantity for assessing the accuracy of crystal structures. *Nature.* 355:472–475.

29. Jones, T.A., J.Y. Zou, S.W. Cowan, and Kjeldgaard. 1991. Improved methods for binding protein models in electron density maps and the location of errors in these models. *Acta Crystallogr. A.* 47:110–119.

30. Laskowski, R.A., M.W. MacArthur, O.S. Moss, and J.M. Thornton. 1993. Procheck: a program to check the stereochemical quality of protein structures. *Journal of Applied Crystallography.* 26:28–29.

31. Brown, J.H., T.S. Jardetzky, J.C. Gorga, L.J. Stern, R.G. Urban, J.L. Strominger, and D.C. Wiley. 1993. Three-dimensional structure of the human class II histocompatibility antigen HLA-DR1. *Nature.* 364:33–39.

32. Ghosh, P., M. Amaya, E. Mellins, and D.C. Wiley. 1995. The structure of an intermediate in class II MHC maturation: CLIP bound to HLA-DR3. *Nature.* 378:457–462.

33. Marsh, S.G.E., and J.G. Bodmer. 1995. HLA class II region nucleotide sequences. *Tissue Antigens.* 45:258–280.

34. Dessen, A., C.M. Lawrence, S. Cupo, D.M. Zaller, and D.C. Wiley. 1997. X-ray crystal structure of HLA-DR4 (DRA*0101, DRB1*0401) complexed with a peptide from human collagen II. *Immunity.* 7:473–481.

35. Busch, R., C.M. Hill, J.D. Hayball, J.R. Lamb, and J.B. Rothbard. 1991. Effect of a natural polymorphism at residue 86 of the HLA-DR β chain on peptide binding. *J. Immunol.* 147:1292–1298.

36. Hammer, J., E. Bono, F. Gallazzi, C. Belunis, Z. Nagy, and F. Sinigaglia. 1994. Precise prediction of major histocompatibility complex class II–peptide interaction based on peptide side chain scanning. *J. Exp. Med.* 180:2353–2358.

37. Hammer, J., F. Gallazzi, E. Bono, R.W. Karr, J. Guenot, P. Valsasnini, Z.A. Nagy, and F. Sinigaglia. 1995. Peptide binding specificity of HLA-DR4 molecules: correlation with rheumatoid arthritis association. *J. Exp. Med.* 181:1847–1855.

38. Fu, X.-T., C.P. Bono, S.L. Woulfe, C. Swearingen, N.L. Summers, F. Sinigaglia, A. Sette, B.D. Schwartz, and R.W. Karr. 1995. Pocket 4 of the HLA-DR(α,β1*0401) molecule is a major determinant of T cell recognition of peptide. *J. Exp. Med.* 181:915–926.

39. Fremont, D.H., W.A. Hendrickson, P. Marrack, and J. Kappler. 1996. Structures of an MHC class II molecule with covalently bound single peptides. *Science.* 272:1001–1004.

40. Fremont, D.H., D. Monnaie, C.A. Nelson, W.A. Hendrickson, and E.R. Unanue. 1998. Crystal structure of I-A^k in complex with a dominant epitope of lysozyme. *Immunity.* 8:305–317.

41. Scott, C.A., P.A. Peterson, L. Teyton, and I.A. Wilson. 1998. Crystal structures of two I-A^d–peptide complexes reveal that high affinity can be achieved without large anchor residues. *Immunity.* 8:319–329.

42. Wucherpfennig, K.W., and J.L. Strominger. 1995. Molecular mimicry in T cell-mediated autoimmunity: viral peptides activate human T cell clones specific for myelin basic protein. *Cell.* 80:695–705.

43. Garboczi, D.N., P. Ghosh, U. Utz, Q.R. Fan, W.E. Biddison, and D.C. Wiley. 1996. Structure of the complex between human T-cell receptor, viral peptide and HLA-A2. *Nature.* 384:134–141.

44. Ding, Y.-H., K.J. Smith, D.N. Garboczi, U. Utz, W.E. Biddison, and D.C. Wiley. 1998. Two human T cell receptors bind in a similar diagonal mode to the HLA-A2/tax peptide complex using different TCR amino acids. *Immunity.* 8:403–411.

45. Hemmer, B., B.T. Fleckenstein, M. Vergelli, G. Jung, H. McFarland, R. Martin, and K.-H. Wiesmüller. 1997. Identification of high potency microbial and self ligands for a human autoreactive class II–restricted T cell clone. *J. Exp. Med.* 185:1651–1659.

46. Gregerson, P.K., J. Silver, and R.J. Winchester. 1987. The shared epitope hypothesis. An approach to understanding the molecular genetics of susceptibility to rheumatoid arthritis. *Arthritis Rheum.* 30:1205–1213.

47. Scharf, S.J., A. Friedmann, C. Brautbar, F. Szafer, L. Steinman, G. Horn, U. Gyllensten, and H.A. Erlich. 1988. HLA class II allelic variation and susceptibility to pemphigus vulgaris. *Proc. Natl. Acad. Sci. USA.* 85:3504–3508.

48. Ahmed, A.R., E.J. Yunis, K. Khatri, R. Wagner, G. Notani, Z. Awed, and C. Alper. 1990. Major histocompatibility complex haplotype studies in Ashkenazi Jewish patients with pemphigus vulgaris. *Proc. Natl. Acad. Sci. USA.* 87:7658–7662.

49. Wucherpfennig, K.W., and J.L. Strominger. 1995. Selective binding of self peptides to disease-associated major histocompatibility complex (MHC) molecules: a mechanism for MHC-linked susceptibility to human autoimmune diseases. *J. Exp. Med.* 181:1597–1601.

50. Fugger, L., J.B. Rothbard, and G. Sonderstrup-McDevitt. 1996. Specificity of an HLA-DRB1*0401–restricted T cell response to type II collagen. *Eur. J. Immunol.* 26:928–933.

51. Rosloniec, E.F., D.D. Brand, L.K. Myers, K.B. Whittington, M. Gumanovskaya, D.M. Zaller, A. Woods, D.M. Altmann, J.M. Stuart, and A.H. Kang. 1997. An HLA-DR1 transgene confers susceptibility to collagen-induced arthritis elicited with human type II collagen. *J. Exp. Med.* 185:1113–1122.

52. Bornstein, M.B., A. Miller, S. Slagle, M. Weitzman, H. Crystal, E. Drexler, M. Keilson, A. Merriam, S. Wassertheil-Smoller, V. Spada, et al. 1987. A pilot trial of Cop 1 in exacerbating-remitting multiple sclerosis. *N. Engl. J. Med.* 317:408–414.

53. Johnson, K.P., B.R. Brooks, J.A. Cohen, C.C. Ford, J. Goldstein, R.P. Lisak, L.W. Myers, H.S. Panitch, J.W. Rose, R.B. Schiffer, et al. 1995. Copolymer 1 reduces relapse rate and improves disability in relapsing-remitting multiple sclerosis: results of a phase III multicenter, double-blind placebo-controlled trial. *Neurology.* 45:1268–1276.

54. Fridkis-Hareli, M., and J.L. Strominger. 1998. Promiscuous binding of synthetic copolymer 1 to purified HLA-DR molecules. *J. Immunol.* 160:4386–4397.

55. Nicholls, A., K.A. Sharp, and B. Honig. 1991. GRASP, computer program. *Proteins.* 11:281–296.

56. Carson, M. 1991. Ribbons 2.0. *Journal of Applied Crystallography.* 24:958–961.